

# Chaos and its quantization in dynamical Jahn-Teller systems

Hisatsugu Yamasaki\* and Yuhei Natsume  
*Graduate School of Science and Technology, Chiba-University  
Inage-ku, Chiba, 263-8522 Japan*

Akira Terai and Katsuhiro Nakamura  
*Department of Applied Physics, Osaka City University  
Sumiyoshi-ku Osaka, 558-8585 Japan*

(Dated: November 21, 2018)

We investigate the  $E_g \otimes e_g$  Jahn-Teller system for the purpose to reveal the nature of quantum chaos in crystals. This system simulates the interaction between the nuclear vibrational modes and the electronic motion in non-Kramers doublets for multiplets of transition-metal ions. Inclusion of the anharmonic potential due to the trigonal symmetry in crystals makes the system nonintegrable and chaotic. Besides the quantal analysis of the transition from Poisson to Wigner level statistics with increasing the strength of anharmonicity, we study the effect of chaos on the electronic orbital angular momentum and explore the magnetic  $g$ -factor as a function of the system's energy. The regular oscillation of this factor changes to a rapidly-decaying irregular oscillation by increasing the anharmonicity (chaoticity).

PACS numbers: 05.45.Mt, 71.70.Ej, 82.90.+j, 03.65.-w, 31.30.Gs

## I. INTRODUCTION

Recently the study on quantization of classically chaotic Hamiltonian systems has received a wide attention. An accumulation of numerical and experimental data indicates Wigner-type level statistics, wavefunction scars and other characteristic features[1, 2].

In addition to toy models like a kicked rotator, Hénon-Heiles system, etc., some realistic systems like a hydrogen atom in a magnetic field and micro-wave cavities are also being investigated[1, 2, 3]. Quantum mechanics of chaotic systems also suggests insight beyond a simple quantal manifestation of chaos[4, 5]. Therefore it is crucial to have more and more experimentally-accessible quantum systems which exhibit chaos in its classical treatment.

In this paper we choose the Jahn-Teller system simulating transition-metal ions embedded in the host crystals such as III-V semiconductors and halides crystals. Among them we consider  $E_g \otimes e_g$  model associated with the irreducible representation for the cubic symmetry group, namely, the two-dimensional (2-d) lattice-vibration modes  $e_g$  linearly coupled to doubly-degenerate electronic states  $E_g$ [6]. This system has an adiabatic doubly-fold lattice potential with the conical intersection of the potential surfaces, whose geometric phase was one of topics some time ago[7, 8]. The lattice potential here can be harmonic or anharmonic. From the classical dynamical viewpoint in the adiabatic limit, as shown below, the system with the 2-d harmonic potential is integrable, leading to regular motions, and on adding the an-

harmonic term, it becomes nonintegrable and chaotic[9]. A systematic investigation of the quantal counterpart of classical chaos in these systems is desirable. Furthermore, since the model is a representative for paramagnetic ions, it is experimentally important to see the effect of chaos on the magnetic  $g$ -factor. This factor is an expectation value for electronic orbital angular momentum and measures a degree of level splitting of highly excited states induced by the lattice-electron interaction. The oscillating structure in energy dependence of  $g$ -factor is expected to reflect the feature of the underlying classical dynamics.

The organization of the paper is as follows: In Section II a model for Jahn-Teller  $E_g \otimes e_g$  system is proposed. Section III deals with the classical analyses of the model. Both the systems with and without anharmonic terms are examined. Section IV presents a quantization of the system together with level statistics. Section V is concerned with a proposal of the experiment to verify the quantum signature of chaos in the dynamical Jahn-Teller system. Some novel feature of  $g$ -factor is explored there. The final Section is devoted to summary and discussions.

## II. DYNAMICAL JAHN-TELLER SYSTEM

We investigate the electronic states of degenerate  $E_g$  orbitals of  $d$ -levels in transition-metal ions coupled with 2-d vibrational modes  $e_g$  expressed by coordinates  $Q_1$  and  $Q_2$ . The  $E_g \otimes e_g$  model is the typical system showing dynamic Jahn-Teller effects (DJTE), which has been discussed in the field of magnetism for transition-metal ions[6, 10]. The Hamiltonian matrix  $H$  for this system is

---

\*Electronic address: hisa@physics.s.chiba-u.ac.jp;  
URL: <http://zeong.s.chiba-u.ac.jp/~hisa/>

expressed as

$$H = -\frac{\hbar^2}{2}\left(\frac{\partial^2}{\partial Q_1^2} + \frac{\partial^2}{\partial Q_2^2}\right)\mathbf{I} + k \begin{bmatrix} Q_1 & Q_2 \\ Q_2 & -Q_1 \end{bmatrix} + V(\mathbf{Q})\mathbf{I}, \quad (1)$$

where  $\mathbf{I}$  is the  $2 \times 2$  unit matrix and  $V(\mathbf{Q})$  is a potential energy. The nuclear mass is set to be unity. The second term of (1) is the so-called Jahn-Teller interaction,  $H_{J-T}$  with  $k$  the coupling parameter between electronic states and vibrational modes. Bases for electronic orbitals  $E_g$  lying behind (1) are  $\langle \mathbf{r}|u \rangle = u(\mathbf{r}) = 3z^2 - r^2$  and  $\langle \mathbf{r}|v \rangle = v(\mathbf{r}) = x^2 - y^2$ . When  $V(\mathbf{Q})$  is a harmonic potential given by

$$V_0(\mathbf{Q}) = \frac{1}{2}\omega^2(Q_1^2 + Q_2^2), \quad (2)$$

the corresponding adiabatic potential for (1) has the Mexican-hut shape in Fig.1, where  $Q_1 = \rho \cos \theta$  and  $Q_2 = \rho \sin \theta$ . The potential minima lie at  $\rho = \rho_0 = k/\omega^2$  with an arbitrary value of  $\theta$ . Namely the minima are infinitely degenerate. The energy for the minima is  $k^2/2\omega^2$ . Vibronic levels for the quantum Hamiltonian (1) were discussed in numerical calculations using small dimensional Hamiltonian matrices[11]. Recently this model has been investigated from a viewpoint of the geometric phase[10, 12]. On the other hand, the effect of the

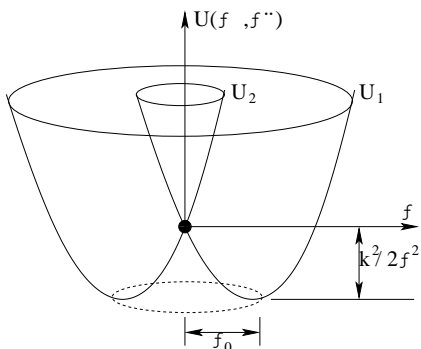


FIG. 1: Adiabatic potential of Mexican-hut shape.  $\rho = \sqrt{Q_1^2 + Q_2^2}$ . The potential has the degenerate minimum.

trigonal fields expressed as the anharmonic term

$$V_A(\mathbf{Q}) = -(b/3)(Q_1^3 - 3Q_1Q_2^2) \quad (3)$$

was also analysed as to some low-lying levels [11, 13]. In short, O'Brien investigated the system (1) with potential  $V(\mathbf{Q}) = V_0(\mathbf{Q}) + V_A(\mathbf{Q})$  in the low-energy approximation that  $\rho$  is fixed to  $\rho_0$ . However, we numerically calculate eigenvalues and eigenvectors without having recourse to such an approximation. We derive level spacing distributions to see the effect of chaos on quantum systems[1, 2, 3, 14, 15, 16]. Furthermore we investigate the quantal  $g$ -factor, whose oscillating structure was shown three decades ago by Washimiya in the system

without anharmonicity. We explore the effect of chaos on the  $g$ -factor in the system with the anharmonicity. The dynamical Jahn-Teller system was also studied by Bulgac and Kusnezov[17, 18, 19, 20] in a system with the three-dimensional harmonic potential. However, we should note that the dimensionality of lattice-vibration modes characterized by the irreducible representation is two and not three according to the theory of a point-symmetry group applied to real crystals and that our model is a better reflection of the real crystal[6].

### III. QUASI-CLASSICAL DYNAMICS AND CHAOS

In the first place, we shall analyze the quasi-classical counterpart of Hamiltonian (1), which is given by

$$H = \frac{1}{2}(P_1^2 + P_2^2) + V(\mathbf{Q}) + k(\mathbf{Q} \cdot \sigma), \quad (4)$$

where the first term is a kinetic energy for classical vibrational modes with coordinates  $\mathbf{Q} = (Q_1, Q_2)$  and the second one is the harmonic and/or anharmonic potential; the third one is the quasi-classical form for the Jahn-Teller interaction where  $\sigma$  is Pauli matrices  $\sigma = (\sigma_x, \sigma_y, \sigma_z)$ . Noting that  $\sigma$  space is independent of the real space, we choose  $\sigma_x, \sigma_y$  and  $\sigma_z$  corresponding to  $\sigma_2, \sigma_3$  and  $\sigma_1$ , respectively. It is convenient to represent the quantum state with use of the density matrix  $\rho$

$$\rho = \frac{1}{2} \begin{pmatrix} 1+z & x-iy \\ x+iy & 1-z \end{pmatrix}, \quad (5)$$

where  $\mathbf{r} = \mathbf{Tr}(\rho\sigma) = (x, y, z) \equiv (\mathbf{r}_\perp, z)$  is a real vector. Using the potential

$$V(\mathbf{Q}) = V_0(\mathbf{Q}) + V_A(\mathbf{Q}) \quad (6)$$

with  $V_0$  and  $V_A$  in (2) and (3), the equations of motion derived from (4) are

$$\frac{d\mathbf{Q}}{dt} = \mathbf{P} \quad (7a)$$

$$\frac{d\mathbf{P}}{dt} = -\frac{dV(\mathbf{Q})}{d\mathbf{Q}} - k\mathbf{r}_\perp \quad (7b)$$

$$\frac{d\mathbf{r}}{dt} = k\mathbf{Q} \times \mathbf{r}. \quad (7c)$$

Equation (7c) is nothing but the Schrödinger equation  $i\dot{\rho} = [H, \rho]$ , from which we find the constant of motion  $|\mathbf{r}| = 1$ . In the study of quasi-classical dynamics, our interest lies in qualitative comparison between the systems with and without the anharmonic term, and therefore we confine to the adiabatic limit  $\frac{dz}{dt} = 0$ , that is,  $\mathbf{r} = (\mathbf{r}_\perp, z_0)$  with  $\mathbf{r}_\perp^2 = 1 - z_0^2$ . Further, we find from (7c),

$$\frac{dz}{dt}\mathbf{e}_z = k\mathbf{Q} \times \mathbf{r}_\perp = 0$$

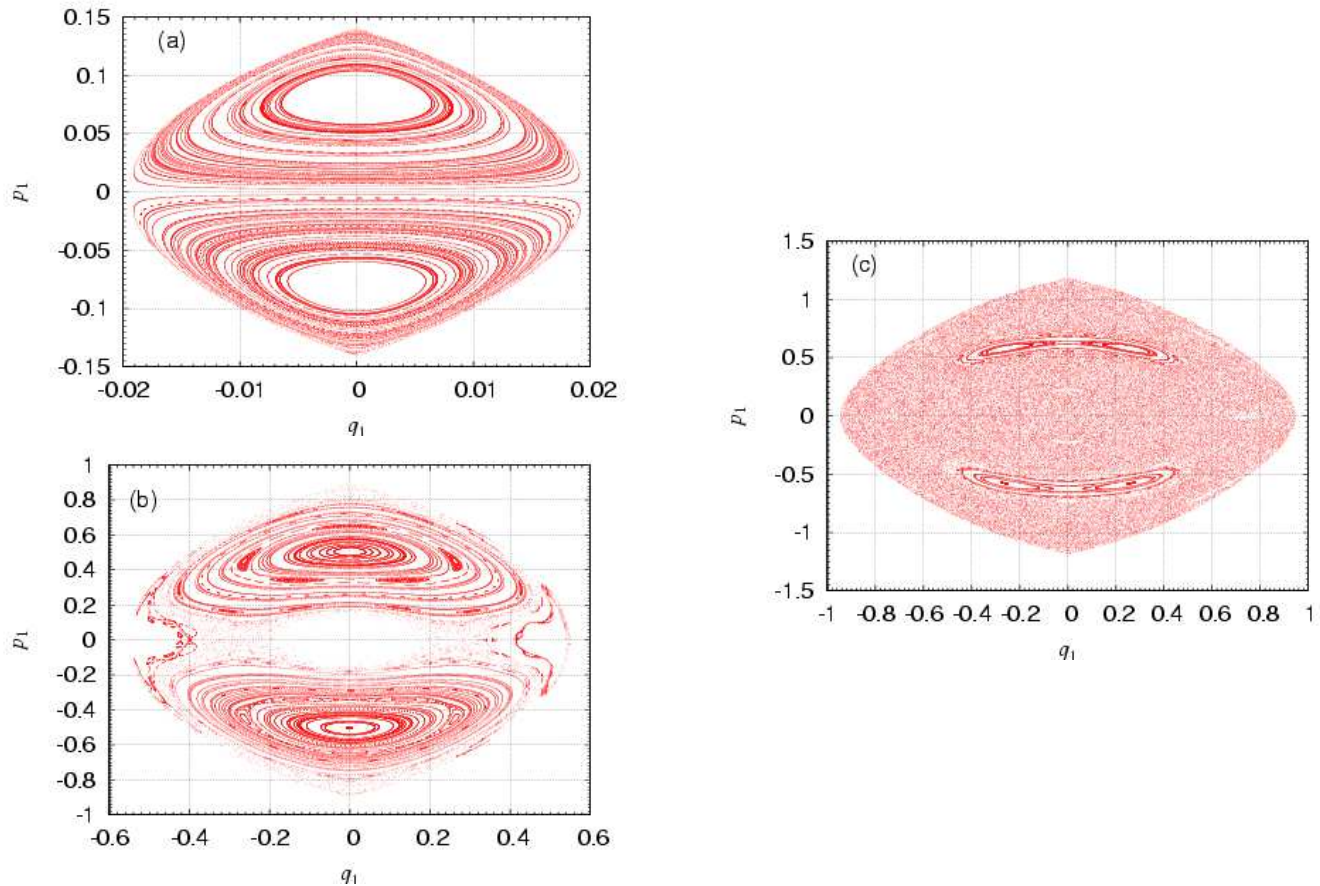


FIG. 2: Poincaré sections at  $p_2 = 0$ .  $\Omega/\omega = 1$ : (a) $\epsilon = 0.01$ , (b) $\epsilon = 0.4$ , (c) $\epsilon = 0.7$ .

which is satisfied only when  $\mathbf{r}_\perp \parallel \mathbf{Q}$ . Thus the adiabatic limit is equivalent to

$$\mathbf{r}_\perp = \sqrt{1 - z_0^2} \frac{\mathbf{Q}}{Q}, \quad (8)$$

where  $Q = |\mathbf{Q}|$ . Thanks to (8), (7b) reduces to

$$\frac{d\mathbf{P}}{dt} = -\frac{dV(\mathbf{Q})}{d\mathbf{Q}} - \tilde{k} \frac{\mathbf{Q}}{Q} \quad (9)$$

with the renormalized coupling  $\tilde{k} = k\sqrt{1 - z_0^2}$ . Consequently, the classical equation of motion for the present model can be expressed only by  $\mathbf{Q}, \mathbf{P}$  and consists of a set of (7a) and (9). This set has the first integral of motion or the total energy

$$E = \frac{\mathbf{P}^2}{2} + V(\mathbf{Q}) + \tilde{k} \frac{\mathbf{Q}^2}{Q}. \quad (10)$$

The following analysis depends on the type of the potential  $V(\mathbf{Q})$ . Firstly, we investigate the system with the harmonic potential only, i.e.,  $V(\mathbf{Q}) = V_0(\mathbf{Q})$ . In this case, in addition to the total energy (10), we have another constant of motion, i.e., the orbital angular momentum

$$J_z = (\mathbf{Q} \times \mathbf{P})_z. \quad (11)$$

The number of constants of motion agrees with the degrees of freedom (two). Therefore the system is integrable [9, 21, 22], showing only regular motions.

Then, we investigate the system with the anharmonic potential  $V(\mathbf{Q}) = V_0(\mathbf{Q}) + V_A(\mathbf{Q})$ . The trigonal field on the 2-d plane  $(Q_1, Q_2)$  is invariant only to operations of the cubic group [6]. Owing to this breaking of continuous circular symmetry, the angular momentum  $J_z$  in (11) is not a constant of motion, which makes the system nonintegrable. It should be noted: the lattice system without coupling with the electronic degree of freedom is identical to the Hénon-Heiles system whose dynamical features have been intensively studied in a context of chaos theory [9, 23].

The present system has two control parameters, i.e., the coupling constant  $\tilde{k}$  between electronic and vibrational degrees of freedom and the nonlinearity parameter  $b$  responsible for the trigonal field. However, the simple scaling below lets them merge to a relevant single parameter. Let the coordinates  $(Q_1, Q_2)$  be transformed to  $(q_1, q_2)$  through  $\sqrt{\frac{b}{k}} Q_1 = q_1, \sqrt{\frac{b}{k}} Q_2 = q_2$ . The total

energy is then written as

$$E = \frac{1}{2} \frac{\tilde{k}}{b} \left( \frac{d\mathbf{q}}{dt} \right)^2 + \frac{\omega^2 \tilde{k}}{2b} \mathbf{q}^2 + \frac{\tilde{k}^{3/2}}{\sqrt{b}} \left[ \frac{1}{2} \sqrt{q_1^2 + q_2^2} + \frac{q_1^3}{3} - q_1 q_2^2 \right]. \quad (12)$$

Next, define the scaled time  $\tau = (\tilde{k}b)^{1/4}t$  and the scaled momentum  $\mathbf{p} = \frac{d\mathbf{q}}{d\tau}$ . Finally, by scaling the energy and the angular frequency as

$$\epsilon = Eb^{1/2}\tilde{k}^{-3/2} \quad (13a)$$

$$\Omega^2 = \omega^2 \tilde{k}^{-1/2} b^{-1/2}, \quad (13b)$$

the total energy is expressed as

$$\epsilon = \frac{1}{2} \mathbf{p}^2 + \frac{1}{2} \Omega^2 \mathbf{q}^2 + \frac{1}{2} \sqrt{q_1^2 + q_2^2} + \frac{q_1^3}{3} - q_1 q_2^2. \quad (14)$$

Eliminating  $\tilde{k}$  between (13a) and (13b), we find  $\epsilon = \left(\frac{\Omega}{\omega}\right)^6 Eb^2$ , which tells that the enhancement of the anharmonic term is equivalent to the increase of the scaled energy  $\epsilon$  under a fixed value of  $\frac{\Omega}{\omega}$ . In our numerics below, we choose  $\frac{\Omega}{\omega} = 1$ . Figure 2 shows Poincaré surface of sections for energies  $\epsilon = 0.01, 0.4$  and  $0.7$ . While in Fig.2(a) we find almost all trajectories to be regular, Fig.2(b) shows that Kolmogorov-Arnold-Moser (KAM) trajectories begin to collapse and some trajectories become chaotic. Finally in Fig.2(c) chaotic trajectories dominate almost all phase space. These results imply that the domain of chaos expands gradually with increasing the scaled energy or the anharmonicity under a fixed value of the scaled angular frequency.

We have also solved Eq.(7) without use of the adiabatic approximation. Then, the degree of freedom becomes three. In case that  $k$  and  $b$  are less than unity, the relative fraction of chaos in phase space is quite small: We call this behavior ‘‘partial chaos’’. However, if both  $k$  and  $b$  are as large as 5, the global chaos as seen in Fig.2(c) appears. In case of  $b = 0$ , we find no indication of irregularity. We shall now proceed to investigate a quantal counterpart of these classical features.

#### IV. QUANTUM SYSTEMS

In this Section we investigate the quantal manifestation of chaos and of regular motions without resorting to the adiabatic limit. The construction of the energy matrix is as follows(see [11] and [24]): The basis wavefunction is described as the products of electronic wavefunctions  $u_{\pm}(\mathbf{r})$  and vibrational ones  $\phi(\mathbf{Q})$ . The former is given in terms of  $u(\mathbf{r})$  and  $v(\mathbf{r})$  below (1) as

$$u_{\pm}(\mathbf{r}) = \frac{1}{\sqrt{2}}(u(\mathbf{r}) \pm iv(\mathbf{r})), \quad (15)$$

while the latter is the eigenstate with the eigenvalue  $E_{nm} = n\hbar\omega$  for the 2-d harmonic oscillator:

$$\phi_{n,m}(\rho, \theta) = F_{n|m}(\rho)e^{im\theta}, \quad (16)$$

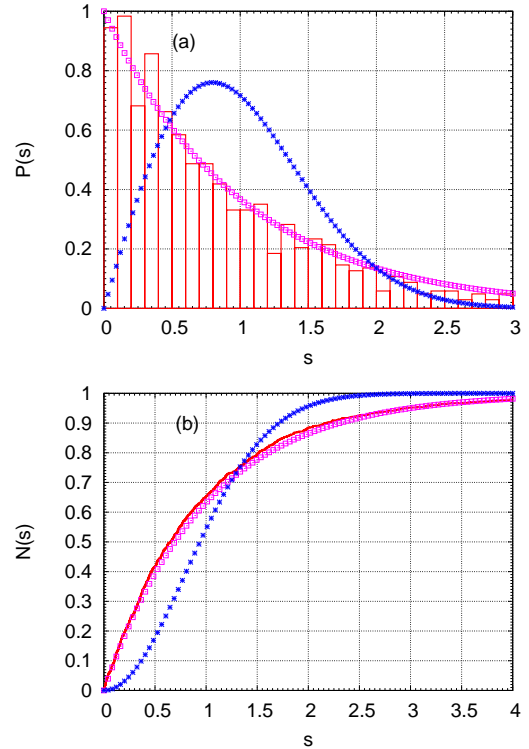


FIG. 3: (a) Histograms of level spacing distribution for  $k = 4, b = 0$ (without trigonal field). Curves of Poisson distribution and GOE are also drawn by open rectangles and crosses, respectively. (b) Integrated level spacing distribution with use of data in Fig.3(a).

where  $n = 1, 2, \dots$ , and  $m = n - 1, n - 3, \dots, -n + 1$ .  $F_{n|m}(\rho)$  is the confluent hypergeometric function[24]. Thus, the basis wavefunctions for the present model are given by

$$\Phi_{n,m}^{\pm} = u_{\pm}(\mathbf{r})\phi_{n,m}(\rho, \theta). \quad (17)$$

Corresponding to (1), the interaction matrix  $H_{J-T}$  is expressed as

$$\begin{aligned} H_{J-T} &= V_u(\mathbf{r})Q_1 + V_v(\mathbf{r})Q_2 \\ &= \frac{\rho}{\sqrt{2}} [V_{u-}(\mathbf{r})e^{i\theta} - V_{u+}(\mathbf{r})e^{-i\theta}] \end{aligned} \quad (18)$$

with the matrix elements of  $V_{u\pm}$  given by

$$\begin{aligned} \langle u_{\pm} | V_{u+}(\mathbf{r}) | u_{\pm} \rangle &= \langle u_{\pm} | V_{u-}(\mathbf{r}) | u_{\pm} \rangle = 0 \\ \langle u_{\mp} | V_{u\pm}(\mathbf{r}) | u_{\pm} \rangle &= \mp \sqrt{2}k. \end{aligned} \quad (19)$$

As for the lattice-vibration factor  $\rho e^{\pm i\theta}$  in (18), we have

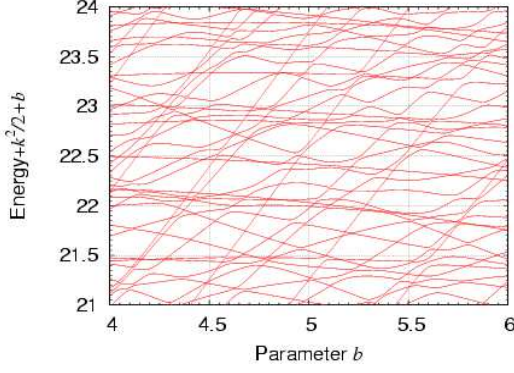


FIG. 4: Dependence of eigenvalues ( $\sim p = 120$ ) on anharmonic parameter  $b$ .

non-vanishing matrix elements as

$$\begin{aligned} \langle \phi_{n,m} | \rho e^{-i\theta} | \phi_{n+1,m+1} \rangle &= \langle \phi_{n+1,m+1} | \rho e^{i\theta} | \phi_{n,m} \rangle \\ &= \left[ \frac{\hbar}{2\omega} (n+m+1) \right]^{1/2}, \\ \langle \phi_{n,m} | \rho e^{-i\theta} | \phi_{n-1,m+1} \rangle &= \langle \phi_{n-1,m+1} | \rho e^{i\theta} | \phi_{n,m} \rangle \\ &= \left[ \frac{\hbar}{2\omega} (n-m-1) \right]^{1/2}. \end{aligned}$$

As a result, the matrix elements for (18) are

$$\begin{aligned} \langle \Phi_{n,m}^+ | H_{J-T} | \Phi_{n',m'}^- \rangle &= k \langle \phi_{n,m} | \rho e^{i\theta} | \phi_{n',m'} \rangle \\ &= k \left\{ \frac{\hbar}{2\omega} [n \pm (m-1)] \right\}^{1/2} \delta_{n',n \mp 1} \delta_{m',m-1} \end{aligned} \quad (20)$$

$$\begin{aligned} \langle \Phi_{n,m}^- | H_{J-T} | \Phi_{n',m'}^+ \rangle &= k \langle \phi_{n,m} | \rho e^{-i\theta} | \phi_{n',m'} \rangle \\ &= k \left\{ \frac{\hbar}{2\omega} [n \pm (m+1)] \right\}^{1/2} \delta_{n',n \pm 1} \delta_{m',m+1}. \end{aligned} \quad (21)$$

If we assign the quantum numbers  $j = \pm 1$  to  $\Phi_{n,m}^\pm$ ,  $H_{J-T}$  without the anharmonic term connects the states with the same quantum number,  $\ell = m - (1/2)j$  ( $j = \pm 1$ ). As discussed by Longuet-Higgins[11], the present matrix decomposes into matrices labeled by quantum number  $\ell$ . For any given value of  $\ell$ ,  $m$  can take two values,  $m = \ell - 1/2$  and  $\ell + 1/2$  corresponding to  $j = -1$  and  $+1$ , respectively. Thus, the  $p$ -th eigenfunction for a given  $\ell$  is expressed as  $\Psi_{p,\ell}$ . If we consider the trigonal field (3), levels with  $\ell \pm 3N$  ( $N = 1, 2, 3, \dots$ ) are coupled to levels of  $\ell$ , as discussed in [11]. The energy matrix is decomposed into only three irreducible presentations,  $A_g$ ,  $B_g$  and  $E_g$ . By the exact diagonalization of each submatrix for the Hamiltonian including  $H_{J-T}$ , we can get eigenvalues and eigenvectors. The result depends on two parameters, the coupling constant  $k$  and the strength of the trigonal field  $b$ . Here, we concentrate on the nearest-neighbor level spacing distribution  $P(s)$ , which plays a prominent role in the quantum description of classically chaotic quantum systems. The random matrix theory presents a natural framework for describing fluctuation properties of spectra of quantum systems, whose corresponding classical

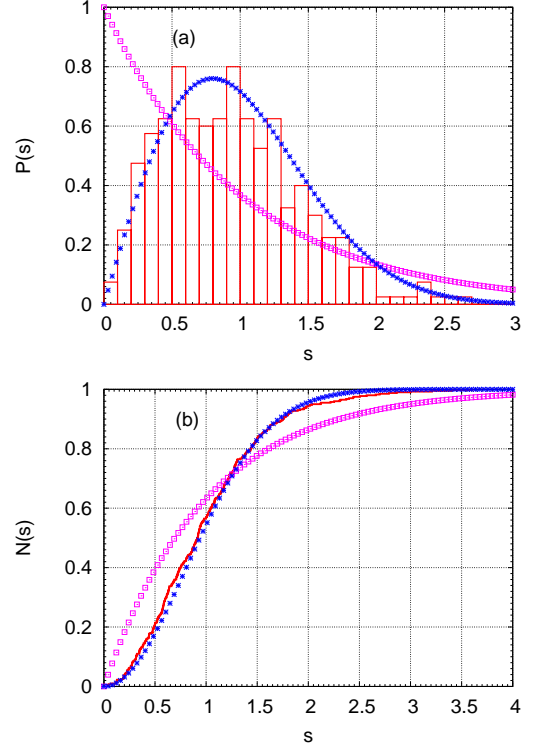


FIG. 5: (a) Histograms of level spacing distribution; (b) Integrated level spacing distribution for  $k = 4, b = 5$  (with trigonal field). Curves of Poisson distribution and Wigner distribution are also drawn by open rectangles and crosses, respectively.

model exhibits chaotic behaviors. In fact the correlations in Gaussian ensembles of random matrices are found to match very closely the empirical correlations among energy levels in classically chaotic systems. If the phase space is totally chaotic, the distribution of level spacings is Wigner-like (GOE),

$$P_w(s) = \frac{\pi}{2} s \exp\left(-\frac{\pi}{4} s^2\right).$$

By contrast, in classically regular quantum systems the levels are independent of each other, and therefore the spacings obey Poisson distribution,

$$P_p(s) = \exp(-s).$$

Considering these standard criteria, we present the level spacing distribution for the Hamiltonian (1) in the following.

First, we consider the system without trigonal field ( $b = 0$ ). For the manifold of  $\ell = 1/2 \pm 3m$  ( $m = 0, 1, 2, \dots$ ), Fig.3(a) shows level spacing distribution characterized by the Poisson distribution, which tells that this system is regular in the classical dynamics[25]. Figure 3(b) shows integrated values of histograms in Fig.3(a), which well fits the function  $1 - e^{-s}$ .

Then we reveal the role of trigonal field. Figure 4 shows

the dependence of eigenvalues on the parameter  $b$ , where a multitude of avoid crossings can be found.

Figure 5(a) shows a level spacing distribution in the case of  $b = 5$ . It should be noted that the distribution perfectly agree with the Wigner one with  $P(s) \rightarrow s$  as  $s \rightarrow 0$ . In Fig.5(b) we show the corresponding integrated level spacing distribution, which also well fits the Wigner one (GOE). We would like to point out the following fact: In the corresponding classical system with  $k = 4$  and  $b = 5$  without use of the adiabatic approximation, the almost whole regions in the phase space exhibit stochastic behavior. However, the system under consideration is generic: the phase space of the underlying classical dynamics consists of both regular Kolmogorov-Arnold-Moser(KAM) tori and chaos. In fact, for smaller values of  $b(0 < b \lesssim 1)$ , we have the Brody distribution interpolating the Poisson and Wigner limits.

While most of studies on quantum chaos have been limited to the analyses of level-spacing distributions and of wavefunctions scars, we shall here embark upon the investigation of experimentally accessible new indicators. We pay attention to magnetism in the dynamical Jahn-Teller system. In particular we discuss the magnetic  $g$ -factor in the next Section[26].

## V. ELECTRONIC ORBITAL ANGULAR MOMENTUM

The essential features of the Jahn-Teller coupled systems are caused by the interaction between the nuclear motions and the electrons in non-Kramers doublets for multiplets of  $d$ -levels. In particular, the quenching of the electronic orbital angular momentum –the so-called magnetic  $g$ -factor– in those doublets is the fundamental subject in magnetism of transition-metal ionic compounds. As well known, the static Jahn-Teller effect removes the ground state degeneracy of electronic states. This effect leads to the complete disappearance of the orbital angular momentum, leaving only spin degree of freedom remains. On the other hands the dynamic Jahn-Teller systems for the relatively weak coupling have a possibility of the nonvanishing orbital angular momentum in non-Kramers doublets because of the continuous distortion of lattices. In fact, in the absence of a trigonal field the  $E_g \otimes e_g$  system has the freedom of the continuous distortion of lattices along the continuous minima of the adiabatic "Mexican hat" potential.

Washimiya[26] payed his attention to the dependence of expectation value of this orbital angular momentum  $\langle L_z \rangle$  in the excited levels  $\Psi_{p,\ell}$  derived in Section IV. He pointed out the oscillatory behavior of  $\langle L_z \rangle$  with increasing energy levels. The non-vanishing values  $\langle L_z \rangle$  are

given as

$$\begin{aligned} \langle L_z \rangle_p &= \langle \Psi_{p,\ell=1/2} | L_z | \Psi_{p,\ell=1/2} \rangle \\ &= \left[ \sum_{n=1}^{\infty} (-1)^n a_{n,p}^2 \right] \Xi, \end{aligned} \quad (22)$$

$p = 1, 2, 3, \dots,$

for the vibronic state of  $\ell = 1/2$ . Here,  $a_{n,p}$ 's are the coefficients of the harmonic oscillator functions. As already mentioned, the vibronic wavefunction is given by

$$\begin{aligned} \Psi_{p,\ell} &= a_{1p} u_-(\mathbf{r}) \phi_{1,0}(\rho, \theta) + a_{2p} u_+(\mathbf{r}) \phi_{2,1}(\rho, \theta) \\ &+ a_{3p} u_-(\mathbf{r}) \phi_{3,0}(\rho, \theta) + a_{4p} u_+(\mathbf{r}) \phi_{4,1}(\rho, \theta) + \dots \end{aligned} \quad (23)$$

In (22),  $\Xi$  is the elements in the principal diagonal of the matrix. ( $\Xi = \langle u_+ | L_z | u_+ \rangle = -\langle u_- | L_z | u_- \rangle$ .) In short, the differences of  $|a_{n,p}|^2$  between even- and odd- numbers of  $n$  in the eigenfunction labeled by  $p$  play an essential role. As  $p$  increases, the oscillatory behavior of the angular momentum is found. The periods of this oscillation are far long in comparison with the variation by odd and even numbers for the small coupling  $k$ . With increasing  $k$ , the absolute value of the angular momentum decreases. The origin of this oscillation has not been clarified up to now, though Washimiya's finding is essential for understanding properties of this vibronic systems.

In what follows, we show a more detailed calculation of this oscillatory behavior. Furthermore, the effect of the trigonal field is discussed in consideration that this field destroys the continuous circular symmetry and that the angular momentum  $\ell$  is not a good quantum number. Under that condition, we introduce the density of  $g$ -factor  $g(\varepsilon)d\varepsilon$  for the electronic orbital angular momentum in the energy range between  $\varepsilon$  and  $\varepsilon + d\varepsilon$  as

$$g(\varepsilon)d\varepsilon = \sum_p' \left| \sum_{n=1}^{\infty} (-1)^n a_{\ell=1/2,n,p}^2 \right| d\varepsilon. \quad (24)$$

Here, the summation of  $p$  is taken over the corresponding energy range. It should be noted that levels for  $\ell' = 1/2 \pm 3N(N = 1, 2, \dots)$  are mixed with the levels for  $\ell = 1/2$  in the presence of the trigonal field.

We show calculated results of  $g(\varepsilon)$  at  $k = 0.707$  in Fig.6: In Fig.6(a), the regular oscillatory behavior of  $g(\varepsilon)$  for  $b = 0$  as a function of level  $p$ , which was reported by Washimiya[26] three decades ago, is reproduced. In addition to histograms for  $g(\varepsilon)$ , we also show the envelop-functions constructed by Gaussian coarse-graining of each peak. Figures 6(b),(c) and (d) show the  $\varepsilon$  dependence of  $g(\varepsilon)$  in the presence of trigonal field with  $b = 0.2, 0.3$  and  $1.41$ , respectively. Here, we can find the suppression of regular oscillation with increasing  $b$ .

The emergence of irregular oscillation and the suppression of  $g$ -factor with increasing  $b$  reflect the underlying chaotic behavior in Section III. We find the important fact: while the level statistics can reach the Wigner distribution for sufficiently-large value  $b$ , the suppression of the



regular oscillation of  $g$ -factor easily occurs for relatively small value  $b$ . In fact the values of  $b = 1.41, k = 0.707$  ( $\Omega/\omega = 1, k \times b = 1$ ) in Fig.6(d) are much less than the values  $b = 5, k = 4$  that guarantee the Wigner distribution in the case without the adiabatic approximation. As a result, the irregular oscillation of  $g$ -factor is a precursor of quantum chaos, namely, the suppression of its regular oscillation occurs even when the classical phase space accommodates a partial chaos.

## VI. SUMMARY AND DISCUSSIONS

We have examined the Jahn-Teller  $E_g \otimes e_g$  system from a viewpoint of classical chaos and its quantization. Both the systems (A) without an trigonal anharmonic term and (B) with it are investigated.

The classical phase space is strictly regular for (A) and nonintegrable and chaotic for (B). In general, the system (B) is mixed of regular KAM tori and chaos. The relative fraction of chaos in the phase space increases as the energy or the strength of the anharmonicity is increased. In the adiabatic approximation, the full chaos can occur easily because of enhancement of non-linear effects due to the strong constraint. Without such an approximation, we can find the full chaos for relatively large values

of  $k$  and  $b$ , and obtain only the partial chaos, if we adopt small values to  $k$  and  $b$ .

For the corresponding quantum systems, the level spacing distributions are shown to be of Poisson and Wigner type for (A) and (B), respectively. We find that the Wigner distribution is available as well by adopting the relatively large values of  $k$  and  $b$ . On the other hand, the dependence of  $g$ -factors on energy  $\varepsilon$  is a quite sensitive indicator of the symptom of chaos in comparison with the level spacing distribution. In the system (A)  $g$ -factor shows regular oscillation with respect to excitation energy. By contrast, in the system (B) it shows a quenched irregular oscillation for the relatively small values of  $k$  and  $b$ . Therefore, we propose the magnetic  $g$ -factor as a new precursor of quantum chaos, superior to the level-spacing distribution. We hope these predictions will be verified in future such as in the experiment of magnetic circular dichromism.

It will be quite important that the precursor of chaos shows up in the observable orbital angular momentum in the dynamical Jahn-Teller systems for transition-metal ionic-compounds. There are other interesting themes in this system, such as an effect of the chaos on a spectral feature of phonon side bands, which will also be examined in due course.

- 
- [1] H.-J. Stöckmann, *Quantum Chaos an introduction* (Cambridge University Press, 1999).
  - [2] F. Haake, *Quantum Signatures of Chaos* (Springer, Berlin, 1991).
  - [3] R. Blümel and W.P. Reinhardt, *Chaos in Atomic Physics* (Cambridge University Press, 1997).
  - [4] K. Nakamura, *Quantum versus Chaos* (Kluwer Academic Publishers, 1997).
  - [5] K.F. Berggren and S. Åberg, *Quantum Chaos Y2K: Proceedings of Nobel Symposium* (Royal Swedish Academy of Science/ World Scientific, Singapore, 2001).
  - [6] S. Sugano, Y. Tanabe, and H. Kamimura, *Multiplets of Transition-Metal Ions in Crystals* (Academic Press, 1970).
  - [7] M.V. Berry, Proc. R. Soc. Lond. **392**, 45 (1984).
  - [8] A. Shapere and F. Wilczek, *Geometric Phase in Physics* (WorldScientific, Singapore, 1989).
  - [9] A.J. Lichtenberg and M.A. Lieberman, *Regular and Chaotic Dynamics* (Springer-Verlag, Berlin, 1990).
  - [10] H. Koizumi and I.B. Bersuker, Phys. Rev. Lett. **83**, 3009 (1999).
  - [11] H.C. Longuet-Higgins, U. Öpik, and M.H.L. Pryce, Proc. Roy. Soc. A. **244**, 1 (1958).
  - [12] C.A. Mead, Rev. Mod. Phys. **64**, 51 (1992).
  - [13] M.C.M. O'Brien, Proc. Roy. Soc. A. **281**, 323 (1964).
  - [14] M.L. Mehta, *Random Matrices* (Academic Press, 1967).
  - [15] O. Bohigas, M.J. Giannoni, and C. Schmit, Phys. Rev. Lett. **52**, 1 (1984).
  - [16] T. Takami and H. Hasegawa, Phys. Rev. Lett. **68**, 1084 (1992).
  - [17] A. Bulgac, Chaos Solitons & Fractals. **5**, 1051 (1995).
  - [18] A. Bulgac, Phys. Rev. A. **37**, 4084 (1988).
  - [19] A. Bulgac and D. Kusnezov, Ann. Phys. **199**, 187 (1990).
  - [20] D. Kusnezov, Phys. Rev. Lett. **72**, 1994 (1994).
  - [21] K. Nakamura, *Quantum Chaos - A New Paradigm of Non-Linear Dynamics* (Cambridge University Press, 1993).
  - [22] V.I. Arnold, *Mathematical Methods of Classical Mechanics* (Nauka, Moscow, 1974).
  - [23] M. Brack and R.K. Bhaduri, *Semiclassical Physics* (Addison-Wesley Pub., 1997).
  - [24] L. Pauling and E.B. Wilson, *Introduction to Quantum Mechanics* (McGraw-Hill, 1935).
  - [25] M.V. Berry and M. Tabor, Proc. R. Soc. Lond. A. **356**, 375 (1977).
  - [26] S. Washimiya, Phys. Rev. Lett. **28**, 556 (1972).

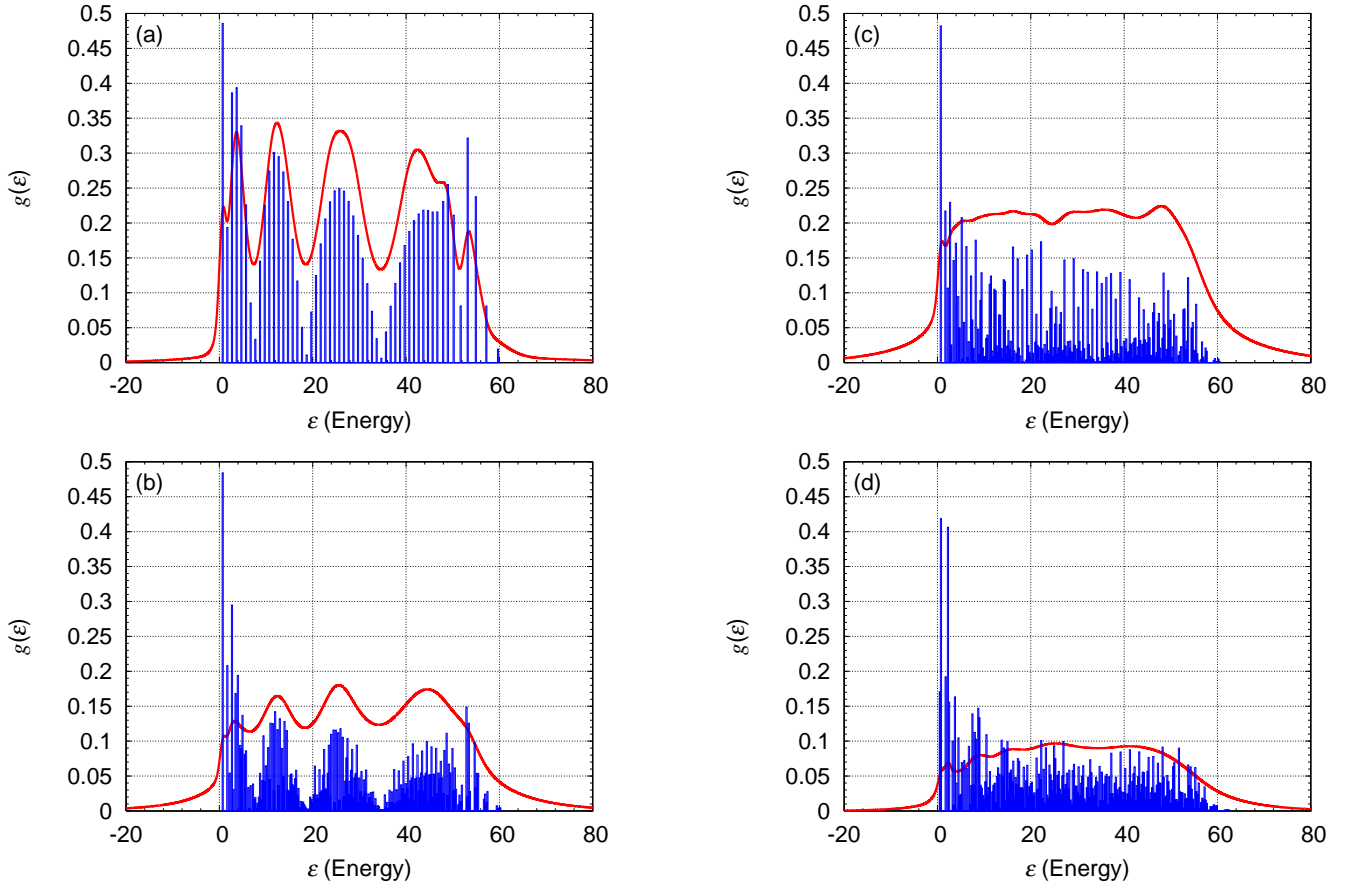


FIG. 6:  $g$ -factor  $g(\varepsilon)d\varepsilon(\varepsilon = 0.25)$  for the electronic orbital angular momentum.  $\ell = 1/2$  and  $k = 0.707$ . (a),(b),(c) and (d) correspond to  $b = 0, 0.2, 0.3$  and  $1.41$ , respectively. Envelop-functions composed for Gaussian distribution types are also depicted.